Crystal and Molecular Structure of (Octaethylporphinato)cobalt(II). Comparison of the Structures of Four-Coordinate M(TPP) and M(OEP) Derivatives (M = Fe–Cu). Use of Area Detector Data

W. Robert Scheidt* and Ilona Turowska-Tyrk[1]

Department of Chemistry and Biochemistry, University of Notre Dame, Notre Dame, Indiana 46556

*Received October 22, 1993**

The crystal and molecular structure of four-coordinate (octaethylporphinato)cobalt(II) has been determined at 127 K from X-ray diffraction data collected on an area detector. Crystals of Co(OEP) are isomorphous with Fe(OEP), one crystalline form of Ni(OEP), and Cu(OEP); the porphinato cores in the series are all planar. The M–N_p bond distance order in the series is Fe > Co > Ni < Cu. The isomorphous M(OEP) derivatives form similar extended π–π aggregates with no metal atom dependence on the intermolecular geometry. A comparison of the analogous, isomorphous series of tetraphenylporphyrin compounds, which have significantly ruffled cores, is given. The average value of the Co–N_p bond distance in Co(OEP) is 1.971 (6). Crystal data: $C_{36}H_{44}N_4Co$, a = 13.046(15) Å, b = 13.217(12) Å, c = 4.742(7) Å, α = 90.60(6)°, β = 92.56(2)°, γ = 113.53(2)°, triclinic, space group $P\bar{1}$, V = 748.5 Å^3, Z = 1, 2640 unique observed data, final data/variable = 14.1, R_1 = 0.039, R_2 = 0.044, all observations at 127 K.

Introduction

The exploration of the basic coordination chemistry and structural properties of metalloporphyrin derivatives has been largely carried out with synthetic porphyrin derivatives rather than the naturally occurring macrocycles. The reasons are manifold but include issues of availability, solubility, photochemical sensitivity, and synthetic considerations. The most prominent synthetic derivatives, chosen primarily for their convenient and desirable physical properties and ease of synthesis, are the *meso*-tetraaryl derivatives, most commonly *meso*-tetraphenylporphyrin (H_2TPP), and the β-pyrrole-substituted compound octaethylporphyrin (H_2OEP).[2] The simplest metallo derivatives are the four-coordinate species M(P), and structures of the Fe(TPP) through Cu(TPP) derivatives have been known for some time.[3–8] However, for H_2OEP derivatives, only Ni(OEP) (two crystalline forms) had been structurally characterized until fairly recently.[9,10] The structure of Fe(OEP) was reported in 1985,[11] a third crystalline form of Ni(OEP) in 1988,[12] and the structure of Cu(OEP) in 1991.[13] We report in this paper the crystal and molecular structure of the last remaining OEP derivative in the series, namely Co(OEP). We compare the structural trends within each M(P) series (P = OEP or TPP) and an important difference between the two series.

The determination of the X-ray structure of Co(OEP) results, at least in part, from access to new diffraction instrumentation that promises to yield greater sensitivity and speed of data collection compared to standard diffractometry intensity measurements. The new instrumentation makes use of area detector technology for the estimations of the X-ray intensities in an accurate and exceptionally rapid manner. Although not an issue for the data collection of Co(OEP), the instrument provides significant enhancements for measurements on compounds with unusually large unit cells; large unit cells are at least an occasional difficulty in metalloporphyrin structure determinations. Since area detector data collection methods for small molecule crystallography are not yet common practice, we will detail our operating procedures with this instrumentation that we expect will describe our general experimental procedures for X-ray intensity collection for a substantial period into the future.

Experimental Section

Co(OEP) was prepared by standard metal insertion procedures.[14] Attempts to prepare X-ray quality crystals, using a number of different procedures, failed to yield adequate single crystals. Small single crystals, in the form of black needles, were eventually prepared by the very slow evaporation of methylene chloride solutions of Co(OEP). The largest single crystal that could be obtained from this procedure was a needle with approximate dimensions of ≤0.03 × 0.1 × 0.7 mm.

This crystal was mounted along the needle direction and subjected to preliminary examination on an Enraf-Nonius FAST[15] area detector system equipped with a molybdenum rotating-anode generator with a 300-μm focal spot, graphite monochromator, κ-axis goniometer, and an Enraf-Nonius low-temperature cooling device operating at 127 K and interfaced to a DEC VAX Model 3400 computer. Instrument control is provided through the Enraf-Nonius PHASE program which interfaces to the program MADNES[16] for crystal setup, unit cell determination and refinement, experiment monitoring, and data collection and reduction.[17] After the crystal is centered on the instrument, the real-time detector system allows

* Abstract published in *Advance ACS Abstracts*, March 1, 1994.

(1) On leave from Department of Chemistry, University of Warsaw, Warsaw, Poland.

(2) Abbreviations used in this paper: OEP, TPP dianions of octaethylporphyrin and *meso*-tetraphenylporphyrin, respectively; P, generalized porphyrin dianion.

(3) Collman, J. P.; Hoard, J. L.; Kim, N.; Lang, G.; Reed, C. A. *J. Am. Chem. Soc.* **1975**, *97*, 2676.
(4) Madura, P.; Scheidt, W. R. *Inorg. Chem.* **1976**, *15*, 3182.
(5) Stevens, E. D. *J. Am. Chem. Soc.* **1981**, *103*, 5087.
(6) (a) Kon H. Personal communication. (b) See also: Sato, M.; Kon, H.; Akoh, H.; Tasaki, A.; Kabuto, C.; Silverton, J. V. *Chem. Phys.* **1976**, *16*, 405.
(7) (a) Hoard, J. L. Private communication. (b) Hoard, J. L. In *Porphyrins and Metalloporphyrins*; Smith, K. M., Ed.; Elsevier: Amsterdam, 1975, Chapter 8.
(8) Fleischer, E. B.; Miller, C. K.; Webb, L. E. *J. Am. Chem. Soc.* **1964**, *86*, 2342.
(9) Meyer, E. F., Jr. *Acta Crystallogr., Sect. B* **1972**, *B28*, 2162.
(10) Cullen, D. L.; Meyer, E. F., Jr. *J. Am. Chem. Soc.* **1974**, *96*, 2095.
(11) Strauss, S. H.; Silver, M. E.; Long, K. M.; Thomspon, R. G.; Hudgens, R. A.; Spartalian, K.; Ibers, J. A. *J. Am. Chem. Soc.* **1985**, *107*, 4207.
(12) Brennan, T. D.; Scheidt, W. R.; Shelnutt, J. A. *J. Am. Chem. Soc.* **1988**, *110*, 3919.
(13) Pak, R.; Scheidt, W. R. *Acta Crystallogr., Sect. C* **1991**, *C47*, 431.
(14) Adler, A. D.; Longo, F. R.; Kampas, F.; Kim, J. *J. Inorg. Nucl. Chem.* **1970**, *32*, 2443.

(15) FAST is an acronym for fast-scanning area sensitive television detector system.

(16) Pflugrath, J.; Messerschmitt, A. MADNES, Munich Area Detector (New EEC) System, version EEC 11/09/89, with enhancements by Enraf-Nonius Corp., Delft, The Netherlands. A description of MADNES is given in: Messerschmitt, A.; Pflugrath, J. *J. Appl. Crystallogr.* **1987**, *20*, 306.

(17) Dr. A. I. Karaulov assisted us in our early use of the FAST and associated software by kindly providing a number of predefined procedures.

0020-1669/94/1333-1314$04.50/0

us to quickly assay crystal quality by examining the digitally measured and stored diffraction images on a monitor. The monitor images resemble those obtained by photographic methods although they are available much more quickly. A typical experiment for crystal quality consists of a 3°–30-s rotation about an arbitrary axis to yield a diffraction image. Most crystalline sample difficulties are apparent at this stage. An estimate of appropriate generator power settings[18] can be made at this stage.

Preliminary unit cell determinations are usually carried out by collecting two 5° ω data scans separated by 90° in ω. For ambient temperature experiments these ω rotations are made with the goniometer head at $\kappa = 0°$. For low-temperature experiments, the cold stream flow would be collinear with the main (ϕ) axis of the goniometer head. To eliminate possible crystal alignment difficulties engendered by differential, time-dependent cooling of the head, the goniometer head is offset by 45° from the normal to the equatorial plane, followed by two ω-axis rotations. Under these conditions, the crystal but not the goniometer head is cooled. The number of reflection positions found in these two scans depends on the size of unit cell, crystal quality, the setting angle of the detector arm, and the detector to crystal distance. The conventional settings (for use with data collection) of the detector angle and distance are –25° and 40 mm, respectively. These settings allow measurement of reflections to 2θ limits greater than the limiting copper sphere (54.86°).[19] Because many diffraction events are occurring simultaneously, typically more than 300 reflections are collected at this stage. Up to 50 of these reflections are used in the autoindexing routine ENDEX, which allows determination of preliminary unit cell constants and lattice type in a way similar to that used on a CAD4. Refined unit cell constants are determined by least-squares refinement of the positions of up to 250 reflections found in these data scans. The three-dimensional reflection positions are defined by the center of Y and Z positions on the face of the area detector (the array is 512 × 512 pixels and dimensions $Y = 62.4$ mm and $Z = 46.8$ mm) and the rotation position of the image. The rotation position is defined by the ω rotation increment. The usual value is 0.2°; larger (smaller) values are chosen for data collection when the sample crystal has high (low) mosaicity. Accordingly, an estimate of crystal mosaicity is made during this least-squares refinement. Refined values of the detector distance and angle are also obtained at this time. Before continuing on to data collection, the proposed crystal system, symmetry conditions, and unit cell lengths are easily confirmed by the collection of axial (oscillation) "photos" for each of the three cell axes (and cell diagonals if needed). These images can be viewed immediately and then stored on computer disk (approximate image size is 525 000 bytes) for subsequent referral. We have also found that crystalline samples with high mosaicities, reflections having asymmetric profiles, or anisotropically varying profiles, all commonly observed conditions for metalloporphyrin crystals, require some additional procedures in order to obtain accurate cell constants. In our procedure we increase the spatial resolution of the diffracted intensity profiles by using a larger crystal to detector distance (80 mm) and a θ angle of 0°. Usually three or four 10° ω data scans, each separated by 45° in ϕ, are employed in obtaining intensities for use in the least-squares refinement. We exclude the very low-angle data ($2\theta < 10°$) and accept all remaining data ($2\theta \leq 24°$). Agreement on all crystalline specimens we have compared is excellent; the procedure gives similar agreements for a wide range of crystal qualities.[20] Cell constants and crystal system thus determined for Co(OEP) are reported in Table 1; the complex is isomorphous with the triclinic B phase of Ni(OEP).[12]

Images for intensity data collection are made by making a series of "sweeps" at the previously selected detector angle and distance (vide supra). Two parameters must be chosen for the sweeps: an integration time for each image and an ω width for each image. Our default values are 10 s and 0.2°, respectively; for weakly scattering crystals the integration time can be increased as well as enhancing the X-ray flux at the crystal by boosting the power settings of the generator. For most crystals we use power settings of 50 kV and 40 mA and an anode rotation speed of 3000 rpm. Four sweeps are then collected: a sweep of 100° rotation of ω at $\kappa = 0°$ (45° offset for low-temperature measurements), a change in ϕ by 90°, a second sweep of 100° rotation of ω, and a setting of $\kappa = 134°$ ($\chi = 90°$), followed by a "cusp" sweep of 73° in ω, a change in ϕ by 90°, and a second cusp sweep of 73° in ω. This procedure provides for the measurement of approximately 1.2 hemispheres of intensity data for any crystal orientation. Even for a triclinic unit cell, there is a significant redundancy in reflection intensity measurements. Most redundant measurements are duplicates, but up to five to seven measurements of a single reflection are made. Validity of reflection positions are continuously monitored during data collection by checking the observed and calculated central position of the reflections—the positions must be within two ω rotation increments or the reflection is flagged; similar constraints are placed on the Y and Z area detector directions. Whenever the center pixels of a reflection overflow their frame (are too intense), the frame is automatically recollected and measured with a lowered gain (sensitivity) setting on the detector. This is the logical equivalent of a beam attenuator: for the current FAST instrument the maximum "attenuator" constant is 52.53. We attempted to choose conditions that lead to a substantial majority of the frames being recollected in order to maximize the number of weaker, high-angle reflections that are reliably measured while not overflowing the detector range for the high intensity reflections.[22] For these data collection conditions, an entire data set can be collected in 6–12 h (elapsed time). For crystals of very unstable substances, these times could clearly be substantially reduced.

The raw data images are transferred via DECNET, immediately after measurement, to a 2.1 GB disk on a VAXstation 4000 Model 90 (disk is large enough to hold the image files from all four sweeps even when all frames have been rescanned). These data images are then evaluated by an off-line version of MADNES. Individual reflection evaluation is based on a best-fit ellipsoid which gives the lowest $\sigma(I)/I$ to determine the boundaries of strong reflections both on the detector face and the ω increment. Thus every pixel within a user-defined "shoebox" around the calculated reflection position is given an assignment of peak or background and the pixel intensities appropriately summed. The assignment of shapes and boundaries of weak reflections are based on those of these strong reflections; the full three-dimensional shapes are stored for several regions of the detector area (default is 16 separate regions). This general strategy of differentiating background and peak is well-known from neutron diffraction analysis.[23]

Data processing by MADNES provides corrections for Lp effects and area detector specific factors for each hkl that impinges on the detector window. The MADNES data are then processed with the ABSURD program (I. Tickle, Birbeck College, London, and P. Evans, MRC, Cambridge)[24]

Table 1. Crystallographic Data for Co(OEP)

chem formula: $C_{36}H_{44}N_4Co$	fw = 591.71
$a = 13.046(15)$ Å	space group: $P\bar{1}$ (No. 2)
$b = 13.217(12)$ Å	$T = 127$ K
$c = 4.742(7)$ Å	$\lambda = 0.71073$ Å
$\alpha = 90.60(6)°$	$\rho_{calcd} = 1.30$ g cm^{-3}
$\beta = 92.555(24)°$	$\mu = 0.594$ mm^{-1}
$\gamma = 113.533(18)°$	$R_1{}^a = 0.039$
$V = 748.5(27)$ Å^3	$R_2{}^b = 0.044$
$Z = 1$	

$^a R_1 = \Sigma||F_o| - |F_c||/\Sigma|F_o|$. $^b R_2 = [\Sigma w(|F_o| - |F_c|)^2/\Sigma w(|F_o|)^2]^{1/2}$.

(18) We have used a much wider range of power settings than we used with sealed tube sources. With a 300-μm focal spot (approximately equivalent to that of a sealed "fine-focus" tube) and Mo anode, the usable power range with our crystalline samples is 250 W to 4.5 kW.

(19) Changes in the values of the detector angle and distance settings allow easy modification of X-ray data resolution. This is especially convenient for large units cell and crystals with high mosaicities.

(20) We used as a criterion for accuracy of the cell constants the agreement between the FAST cell and the diffractometer cell determination. In all cases, the same crystalline specimen was used for both determinations. We have made comparisons on 10 different compounds (six metalloporphyrins) with widely varying crystal quality. We note that although the agreements in cell constants are excellent, the cell esd's from the FAST data tend to be larger than those from diffractometer data. The increased values of the esd's range up to 6 times as large although typically the difference is less than a factor of 2. These increased esd's have the effect of causing small increases in values of the esd's on bond distances and angles. Note though that one published comparison[21] of cell constant determinations by independent laboratories suggests that diffractometer cell constant esd's are too small by a factor of 5 to 10.

(21) Taylor, R.; Kennard, O. *Acta Crystallogr., Sect. B* **1986**, *B42*, 112–120.

(22) Data can be collected with one detector setting (distance up to 50 mm) when the cell has a maximum cell length of ~35 Å. This leads to collection of intensity data with $2\theta_{max} \leq 56°$. (At our normal detector distance of 40 mm, $2\theta_{max} \leq 62°$.) Cells with one edge larger than ~35 Å require larger detector distances. In this case, data of lower resolution will be obtained. Alternatively, data collection at two positions of the detector arm can be used to achieve equivalent resolution.

(23) Lehman, M. S.; Larsen, F. K. *Acta Crystallogr., Sect. A* **1974**, *A30*, 580.

(24) Evans, P. R. ABSURD—Absorption correction program for the Area Detector. MRC Laboratory of Molecular Biology, Hills Road, Cambridge, UK, 1990.

using subroutines from the CCP4 suite of programs.[25] ABSURD provides values of F_o and $\sigma(F_o)$ and, using a subroutine written by A. I. Karaulov (University of Wales, Cardiff), examines the entire data set for possible systematic absences, which allows the user to make the space group assignment(s). Estimates of an appropriate cutoff for "observed" diffraction data from the FAST have been made by examining the number of systematic absences remaining at various values of $F_o/\sigma(F_o)$ for a collection of data sets. These results were compared with our experience with serial diffractometer data where we have routinely used the criterion of $F_o \geq 3\sigma(F_o)$ for observed data. From these comparisons, ratios of $F_o/\sigma(F_o) \geq 1.5$–2.0 provides data sets with comparable signal-to-noise as the usual diffractometer data sets. For the Co(OEP) data set, all data with $F_o \geq 2\sigma(F_o)$ were taken to be observed, leading to 5400 observed data.

An indication of data quality is provided by the value of R_{merge} and with the high redundancy available from an area detector should be routinely calculated. The value of R_{merge} for Co(OEP) was 0.027, obtained from the merging of 5400 observed reflections to 2640 symmetry unique data. Although we have not studied the question in a systematic way, the R_{merge}'s obtained from FAST data appear to be smaller than ones we have obtained from data collected on Enraf-Nonius CAD4 and Siemens P$\bar{1}$ diffractometers. It should be noted that the data redundancy allows the ready use of an empirical absorption correction employing the DIFABS logic described by Walker and Stuart.[26] This program has been adapted for area detector geometry by Karaulov.[27]

Initial coordinates for Co(OEP) were taken from the isomorphous Ni(OEP) structure.[12] An isotropic least-squares refinement[28] employing unit weights, followed by anisotropic full-matrix refinement for all non-hydrogen atoms, converged smoothly. Hydrogen atoms were included in the refinement as fixed, idealized contributors (C–H = 0.95 Å, B(H) = $1.2B_{iso}$ (associated C)). The final refinement led to conventional discrepancy indices $R_1 = 0.039$ and $R_2 = 0.044$ for 2640 reflections. The maximum and minimum electron densities in the final difference Fourier map were +0.39 and –0.50 e/Å^3 respectively.

Complete details of the data collection and refinement process are given in Table SI. Final atomic coordinates for Co(OEP) are given in Table 2. Final values of anisotropic thermal parameters are given in Table SII of the supplementary material. As part of our local experimental validation of FAST data collection procedures and strategies, we also collected data on this crystal on a standard serial diffractometer (CAD4) at 293 K and on the FAST instrument at 293 K. Both measurements employed graphite-monochromated Mo Kα radiation. Owing to the small crystal size, the CAD4 data set required 3 full days to collect a unique data data set. A total of 2077 reflections were considered observed and used to refine the structure: final R's were 0.040 and 0.046. The 293 K FAST data set consisted of 2219 unique observed data, again collected within a twelve-hour period: final R's were 0.045 and 0.049. Structural features in the three determinations are not substantially different.

Results

The molecular structure of the centrosymmetric Co(OEP) molecule is illustrated in the ORTEP drawing of Figure 1 which also gives the atom labels for the crystallographically unique half of the molecule. Individual values of bond distances and angles are given in Table 3. The average values of bond parameters (Figure 2) are typical of metalloporphyrins.[29] The two Co–N_p distances are 1.967(3) and 1.975(2) Å. These Co–N_p distances are comparable to the values reported for the known four-coordinate cobalt(II) porphyrins,[4-6,30-32] when core conformation effects are taken into account. Figure 2 displays the deviations, in units of 0.01 Å, of the unique atoms from the mean plane of the 24-atom core; Co(OEP) clearly shows only small variations from exact planarity. Figure 2 also shows averaged values of all bond parameters in the porphinato core; the numbers in parentheses are the estimated standard deviations calculated on the assumption that averaged values are drawn from the same population.

Co(OEP) molecules form an extended one-dimensional array along the crystallographic c axis as shown in Figure 3. The Co···Co separation of 4.74 Å is set by the length of the c axis; the separation between pairs of porphyrin planes is 3.33 Å. The lateral shift between the center of any pair of Co(OEP) molecules along the chain is 3.37 Å. These inter-ring values are those of class I in the categorization of Scheidt and Lee.[33]

Table 2. Fractional Coordinates and Equivalent Temperature Factors[a]

atom	x	y	z	B_{eq},[b] Å^2
Co	0.0000	0.0000	0.0000	1.06
N(1)	0.05706(15)	–0.07051(14)	0.2950(4)	1.22
N(2)	0.12865(15)	0.14173(14)	0.0846(4)	1.22
C(a1)	0.01335(18)	–0.17900(18)	0.3691(5)	1.25
C(a2)	0.15083(18)	–0.02216(18)	0.4718(5)	1.21
C(a3)	0.21540(18)	0.16194(17)	0.2788(5)	1.17
C(a4)	0.15186(18)	0.24022(17)	–0.0449(5)	1.26
C(b1)	0.08085(19)	–0.19982(19)	0.5893(5)	1.37
C(b2)	0.16698(19)	–0.10099(18)	0.6571(5)	1.36
C(b3)	0.29747(19)	0.27416(18)	0.2682(5)	1.41
C(b4)	0.25724(18)	0.32314(17)	0.0672(5)	1.38
C(m1)	0.22470(19)	0.08690(18)	0.4653(5)	1.37
C(m2)	0.08549(19)	0.25821(18)	–0.2521(5)	1.40
C(11)	0.06310(21)	–0.30944(19)	0.7075(5)	1.70
C(12)	0.11833(27)	–0.37135(22)	0.5406(7)	2.47
C(21)	0.26278(22)	–0.07751(20)	0.8638(6)	1.87
C(22)	0.36635(24)	–0.07823(29)	0.7287(8)	2.79
C(31)	0.40621(20)	0.32029(19)	0.4353(6)	1.65
C(32)	0.49198(21)	0.28027(23)	0.3208(7)	2.34
C(41)	0.30841(20)	0.44023(18)	–0.0267(5)	1.65
C(42)	0.26000(23)	0.51453(19)	0.1127(6)	2.09

[a] The estimated standard deviations of the least significant digits are given in parentheses. [b] $B_{eq} = 4[V^2 \det(\beta_{ij})]^{1/3}$.

Discussion

With the structure determination of Co(OEP), the crystal and molecular structure of all M(OEP) and M(TPP) derivatives in the series M = Fe, Co, Ni and Cu have now been determined. The iron(II) derivatives have an intermediate-spin state; all other compounds are low spin. A summary of some aspects of the stereochemistry of the known derivatives for the two porphyrin series is given in Table 4. Each porphyrin ligand set forms an isomorphous series of transition metal derivatives. In addition, within each porphyrin ligand set, there are an additional, but limited, number of polymorphic derivatives.

We first consider the members of the two isomorphic series. The M(OEP) isomorphic series is a group of extended π–π linear aggregates, all of which are found in the triclinic crystal system. All members have planar porphyrin cores. All derivatives also show the pattern depicted in Figure 3; a thorough description of the extended pattern in the solid state has been given previously.[12] The metrical details of the aggregate geometry in the series are constant; there is thus no apparent metal ion dependence. It is

(25) CCP4, 1979, The SERC (UK) Collaborative Computing Project No. 4, a Suite of Programs for Protein Crystallography (distributed from Daresbury Laboratory, Warrington WA 4AD, UK).
(26) Walker, N. P.; Stuart, D. *Acta Crystallogr., Sect. A* **1983**, *A39*, 158.
(27) Karaulov, A. I.; School of Chemistry and Applied Chemistry, University of Wales College of Cardiff, Cardiff CF1 3TB, UK, personal communication.
(28) Programs used in this study included local modifications of Jacobson's ALLS, Zalkin's FORDAP, Busing and Levy's ORFE, and Johnson's ORTEP2. Atomic form factors were from: Cromer, D. T.; Mann, J. B. *Acta Crystallogr., Sect. A* **1968**, *A24*, 321. Real and imaginary corrections for anomalous dispersion in the form factor of the cobalt atom was from: Cromer, D. T.; Liberman, D. J. *J. Chem. Phys.* **1970**, *53*, 1891. Scattering factors for hydrogen were from: Stewart, R. F.; Davidson, E. R.; Simpson, W. T. *J. Chem. Phys.* **1965**, *42*, 3175. All calculations were performed on VAXstation 4000 Model 90 computer.
(29) Hoard, J. L. In *Porphyrins and Metalloporphyrins*; Smith, K. M., Ed.; Elsevier: Amsterdam, 1975; pp 317–380. Scheidt, W. R. In *The Porphyrins*; Dolphin, D., Ed.; Academic Press: New York, 1978; Vol. III, pp 463–511.
(30) Sparapany, J. W.; Crossley, M. J.; Baldwin, J. E.; Ibers, J. A. *J. Am. Chem. Soc.* **1988**, *110*, 4559.
(31) Kim, K.; Collman, J. P.; Ibers, J. A. *J. Am. Chem. Soc.* **1988**, *110*, 4242.
(32) Kadish, K. M.; Araullo-McAdams, C.; Han, B. C.; Franzen, M. M. *J. Am. Chem. Soc.* **1990**, *112*, 8364.
(33) Scheidt, W. R.; Lee, Y. J. *Struct. Bonding (Berlin)* **1987**, *64*, 1.

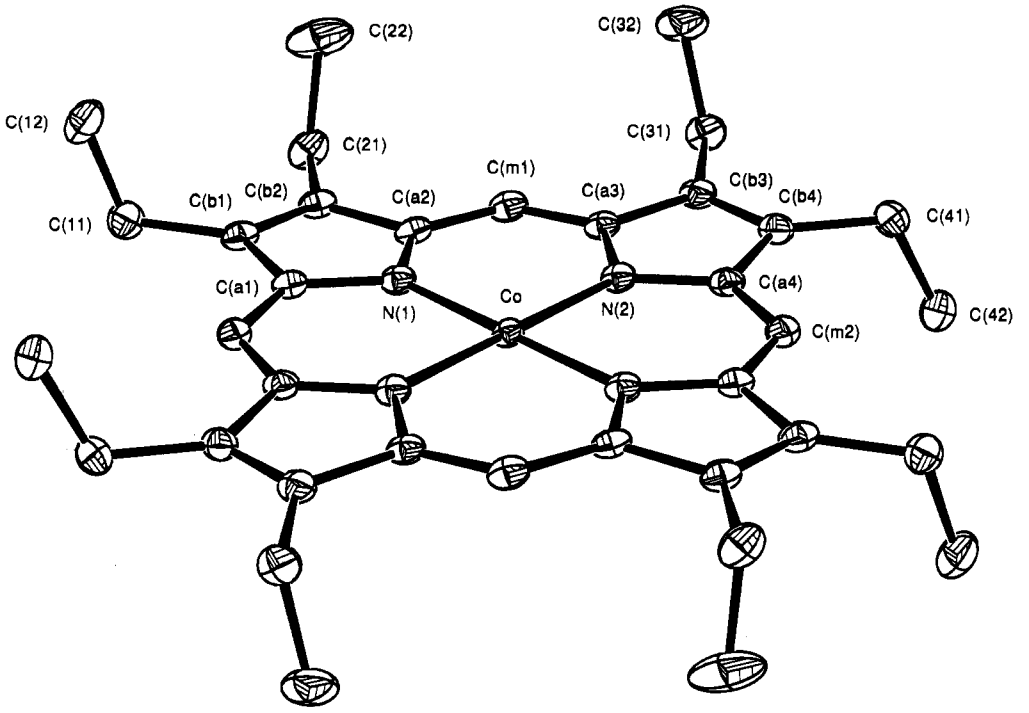

Figure 1. ORTEP diagram of the centrosymmetric Co(OEP) molecule giving the atom labeling scheme used throughout the paper. Atoms are contoured at the 50% probability level. Hydrogen atoms are not shown for reason of clarity.

Table 3. Bond Lengths (Å) and Angles (deg) in Co(OEP)[a]

	A. Bond Lengths		
Co–N(1)	1.9666(27)	C(a3)–C(b3)	1.445(3)
Co–N(2)	1.9749(23)	C(a4)–C(b4)	1.447(3)
N(1)–C(a1)	1.371(3)	C(b1)–C(b2)	1.364(3)
N(1)–C(a2)	1.371(3)	C(b3)–C(b4)	1.357(4)
N(2)–C(a3)	1.364(3)	C(b1)–C(11)	1.493(4)
N(2)–C(a4)	1.372(3)	C(b2)–C(21)	1.481(4)
C(a2)–C(m1)	1.379(3)	C(b3)–C(31)	1.487(4)
C(a3)–C(m1)	1.373(4)	C(b4)–C(41)	1.502(3)
C(a4)–C(m2)	1.366(4)	C(11)–C(12)	1.524(4)
C(a1′)–C(m2)	1.383(3)	C(21)–C(22)	1.524(4)
C(a1)–C(b1)	1.435(4)	C(31)–C(32)	1.532(4)
C(a2)–C(b2)	1.442(4)	C(41)–C(42)	1.523(4)
	B. Bond Angles		
N(1)CoN(2)	90.12(11)	C(b4)C(a4)C(m2)	124.29(22)
N(2)CoN(1′)	89.88(11)	C(a1)C(b1)C(b2)	106.39(22)
CoN(1)C(a1)	128.14(16)	C(a2)C(b2)C(b1)	105.92(23)
CoN(1)C(a2)	127.66(16)	C(a3)C(b3)C(b4)	105.97(21)
C(a1)N(1)C(a2)	104.19(20)	C(a4)C(b4)C(b3)	106.76(21)
CoN(2)C(a3)	127.39(16)	C(a2)C(m1)C(a3)	124.77(23)
CoN(2)C(a4)	127.47(17)	C(a4)C(m2)C(a1′)	125.10(23)
C(a3)N(2)C(a4)	105.11(19)	C(a1)C(b1)C(11)	126.38(22)
N(1)C(a1)C(b1)	111.78(20)	C(b2)C(b1)C(11)	127.15(25)
N(1)C(a1)C(m2′)	124.22(23)	C(b1)C(11)C(12)	112.83(21)
C(b1)C(a1)C(m2)	123.97(22)	C(a2)C(b2)C(21)	125.64(21)
N(1)–C(a2)C(b2)	111.70(20)	C(b1)C(b2)C(21)	128.34(23)
N(1)C(a2)C(m1)	124.73(22)	C(b2)C(21)C(22)	112.78(25)
C(b2)C(a2)C(m1)	123.48(23)	C(a3)C(b3)C(31)	125.13(22)
N(2)C(a3)C(b3)	111.49(21)	C(b4)C(b3)C(31)	128.79(21)
N(2)C(a3)C(m1)	125.18(20)	C(b3)C(31)C(32)	112.30(22)
C(b3)C(a3)C(m1)	123.32(22)	C(a4)C(b4)C(41)	124.91(23)
N(2)C(a4)C(b4)	110.64(22)	C(b3)C(b4)C(41)	128.33(22)
N(2)C(a4)C(m2)	125.07(21)	C(b4)C(41)C(42)	113.01(20)

[a] The numbers in parentheses are the estimated standard deviations.

to be presumed that this geometry is defined by the porphyrin–porphyrin interactions. There is a significant metal ion effect on the M–N_p bond lengths. Within the series, the order is Fe (1.996 Å) > Co (1.971 Å) > Ni (1.952 Å) < Cu (1.998 Å). The bond distance differences primarily reflect the size of the metal ions (vide infra). In the iron[11] and nickel[12] complexes a small but apparently real difference was seen in the two unique M–N_p bond lengths. This difference was ascribed to the effects of

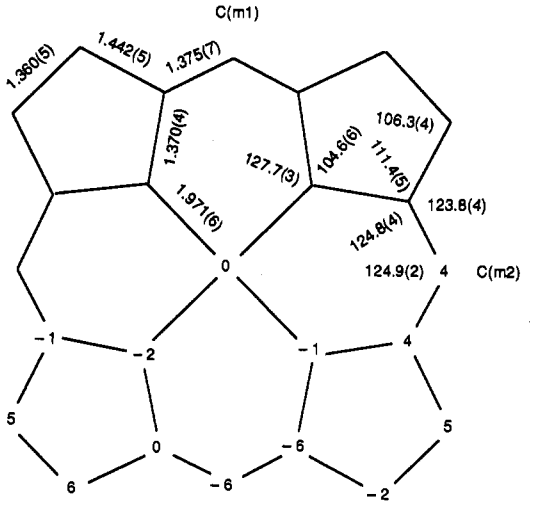

Figure 2. Formal diagram of the porphinato core of the Co(OEP) molecule displaying, on the lower half of the centrosymmetric diagram, the displacement of each unique atom from the 24-atom mean plane. All displacements are given in units of 0.01 Å. Also entered on the diagram are the averaged values of all bond distances and angles of the core.

interporphyrin π–π interactions. These effects on M–N_p bond distance are also seen in the present case but at the 2.3σ level.

The M(TPP) isomorphic series is a set of substantially S_4-ruffled compounds, all in the tetragonal crystal system. The S_4-ruffling of the tetraphenylporphinato core leads to a substantial up–down displacement of the methine carbon atoms of the porphyrin core; the exact values are given in Table 4. Scheidt and Lee[33] have called this pattern "Ruf". Within the isomorphous series, the bond length order is Fe (1.972 Å) > Co (1.949 Å) > Ni (1.928 Å) < Cu (1.981 Å); the series ordering is in *quantitative* as well as qualitative agreement with that observed for the M(OEP) series. The quantitative series ordering as well as the remarkably constant difference of ~0.022 Å in M–N_p distances between each respective element in the M(TPP) vs M(OEP) series emphasizes the importance of metal size and bonding in defining the structures. The shorter bond distances in the M(TPP) series are caused by the well-known effect of porphyrin core

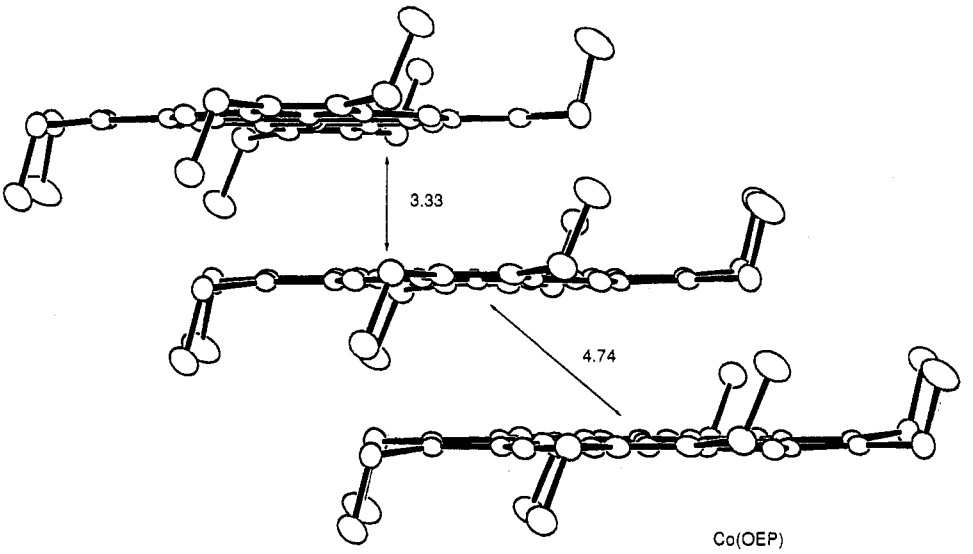

Figure 3. Edge-on view of the Co(OEP) π–π interactions in the solid state. Distances shown are the Co···Co separation and the mean plane separation, which are repeated indefinitely along the chain (*c* axis).

Table 4. Stereochemical Summary for M(OEP) and M(TPP) Complexes

derivative	M–N_p, Å[a]	core conformation[b]	C_m displacement[c]	comment	temp, K	ref
Fe(TPP)	1.972(4)	S_4-ruffled (Ruf)	●40	tetragonal	292	3
Fe(OEP)	1.996(16)	planar	±2	triclinic, π–π stack	293	11
Co(TPP)	1.949(3)	S_4-ruffled (Ruf)	±42	tetragonal	293	4
	1.949(1)	S_4-ruffled (Ruf)	±42	tetragonal	100	5
	1.951(1)	S_4-ruffled (Sad)	0	triclinic	RT	6
Co(OEP)	1.971(6)	planar	±6, ±4	triclinic, π–π stack	127	this work
Ni(TPP)	1.928(3)	S_4-ruffled (Ruf)	±45	tetragonal	292	7
Ni(OEP)	1.929(3)	S_4-ruffled (Ruf)	±51	tetragonal	293	9
	1.958(4)	planar	±2	triclinic A	RT	10
	1.952(8)	planar	±6, ±1	triclinic B, π–π stack	294	12
Cu(TPP)	1.981(7)	S_4-ruffled (Ruf)	±42	tetragonal	RT	8
Cu(OEP)	1.998(2)	planar	±4, ±1	triclinic, π–π stack	293	13

[a] Number in parentheses is the estimated standard deviation of an individual value (tetragonal Ni(OEP) and all M(TPP)'s, except the second value for Co(TPP)) or the esd of the average (all remaining M(OEP)'s and the second Co(TPP) value). [b] The S_4-ruffling geometries "Ruf" and "Sad" have been defined by Scheidt and Lee.[33] [c] Deviations given in units of 0.01 Å from the 24-atom mean plane.

ruffling that was first quantitatively described by Hoard.[34] It is interesting to note however, that the four M(TPP) derivatives exhibit almost exactly the same degree of ring ruffling, as measured by the C_m displacement, despite the differences in the M–N_p bond distances. This latter observation suggests that the S_4-ruffling of the M(TPP) cores has, at the least, a substantial component caused by solid-state packing of the molecules. The nearly constant difference in M–N_p bond distances of the planar M(OEP) vs the respective ruffled M(TPP) derivative is an important observation that shows the limitations of modifying core conformations on M–N_p distances, at least with the biologically significant first-row transition elements.

Finally, we consider the members that are not part of the respective isomorphous series. In the M(TPP) series, the additional member is a second form of Co(TPP).[6] It exhibits an alternative pattern of S_4-ruffling in which the methine carbons are not displaced from the mean plane of the porphyrin core but instead only pyrrole ring atoms are displaced. In this arrangement, both β-carbons on each pyrrole ring are alternately displaced equally up or down (the "Sad" geometry).[33] In the M(OEP) series, there are two other crystalline forms of Ni(OEP), a ruffled form[9] and a planar one (triclinic A).[10] The ruffled form shows a significantly decreased Ni–N_p bond distance. In this laboratory, we[12] have only been able to isolate the triclinic A planar form when the crystallizing medium also contains a small amount of H_2OEP impurity. Indeed, the triclinic A form is isomorphous with H_2OEP.[35] We presume that the function of the H_2OEP impurity is to form nucleation sites for subsequent Ni(OEP) deposition. This tactic (added H_2OEP impurity) has also allowed us to the isolation of small crystals of the triclinic A form of Cu(OEP),[36] although a crystal structure analysis has not been performed.

In conclusion, we have reported the structure of the last remaining derivative, Co(OEP), in the M(OEP) (M = Fe–Cu) series. The M(OEP) and M(TPP) derivatives show quantitative and qualitative trends in the M–N_p bond lengths in the series. The differences reflect both the effects of the metal ion and the core conformation. The strongly displayed differences in the porphyrin core conformation may indicate that there are energetic differences in nonplanar deformations between the two series with planarity being favored for the M(OEP) series.

Acknowledgment. We thank the National Institutes of Health for support of this research through Grants GM-38401 and RR-06709, Roger Pak for many crystal growing experiments and Dr. M. Shang for the CAD4 data collection. W.R.S. acknowledges the hospitality and patience of Prof. Michael Hursthouse and Drs. Christian Lehman and A. I. (Sacha) Karaulov of University of Wales, Cardiff College, for FAST tutorials, explanations, and other assistance.

Supplementary Material Available: Table SI, containing complete crystallographic details, Table SII, containing thermal parameters, and Table SIII, containing fixed hydrogen atom positions (3 pages). Ordering information is given on any current masthead page.

(34) Hoard, J. L. *Ann. N. Y. Acad. Sci.* **1973**, *206*, 18.
(35) Lauher, J. W.; Ibers, J. A. *J. Am. Chem. Soc.* **1973**, *95*, 514.
(36) Sparks, L. D.; Scheidt, W. R.; Shelnutt, J. A. *Inorg. Chem.* **1992**, *31*, 2191.